Immersion and Invariance Adaptive Visual Servoing of Manipulators with Uncertain Dynamics

Alessandro R. L. Zachi, Liu Hsu, Romeo Ortega and Fernando Lizarralde

Abstract— **The problem of direct adaptive visual servoing of robot manipulators is considered. A solution is developed for image-based look-and-move visual systems to allow tracking of a desired trajectory, when both camera calibration and robot dynamics are uncertain. In order to solve the multivariable parameter adaptive problem, the recently proposed Immersion and Invariance (I&I) method is used. The scheme is then combined with a robust motion controller for the manipulator, which takes into account its uncertain nonlinear dynamics and leads to an overall stable adaptive visual servoing system. The effectiveness of the proposed strategy is illustrated through simulations and experimental results.**

Index Terms— **Nonlinear control, adaptive control, visual servoing, uncertain robotic systems**

I. INTRODUCTION

Robotic visual servoing techniques have been studied for many years and has still received considerable attention in the recent robotics literature as potential tools for relevant industrial and also medical sensor-based robotic applications [10]. As part of this trend, the problem of tracking a desired trajectory based on the image features has been explored in several works as a control-theoretic issue [5], [15], [12], [14], [16], [18]. The uncertainties of model parameters have been of concern since the early developments. Several adaptive schemes have been proposed to circumvent the performance degradation due to modeling uncertainty, particularly with respect to the camera calibration and robot parameters. Among the early works in this field we cite [3], [7], [19], [20], [22]. However, most of the above cited works have not considered the non-linear robot dynamics in the controller design. These controllers may result in unsatisfactory performance when high-speed tasks or direct-drive actuator are required. Exceptions can be found in recent papers like [9], [11], [13], [14], [21], [23].

In this paper we propose a solution for the direct adaptive visual tracking of planar manipulators using a fixed camera, when both camera calibration and robot dynamics are uncertain. The proposed strategy is developed for image-based look-and-move visual servoing systems. In order to solve the multivariable parameter adaptive problem related to the camera calibration uncertainty, the recently proposed Immersion and Invariance (I&I) method [22] is used. One of the advantages of the I&I is to avoid controller over-parametrization in the visual servo loop [20]. The scheme is then combined with a robust controller for the manipulator based on sliding mode control [4], which takes into account its nonlinear dynamics and lead to an overall globally stable adaptive system. Simulation and experimental results are also presented to illustrate the effectiveness of the proposed scheme.

This work was partially supported by CNPq and FAPERJ.

Alessandro R. L. Zachi is with the Department of Electrical Engineering, Centro Federal de Educação Tecnológica Celso Suckow da Fonseca, Rio de Janeiro, Brazil. zachi@coep.ufrj.br

Liu Hsu is with the Department of Electrical Engineering/COPPE, Federal University of Rio de Janeiro, Rio de Janeiro, Brazil. liu@coep.ufrj.br

Romeo Ortega is with the Laboratoire des Signaux et Systémes, Supelec, Gif-sur-Yvette, France. romeo.ortega@lss.supelec.fr

Fernando Lizarralde is with the Department of Electronic Engineering, and Department of Electrical Engineering/COPPE, Federal University of Rio de Janeiro, Rio de Janeiro, Brazil. fernando@coep.ufrj.br

II. PROBLEM FORMULATION

Consider the problem of tracking a desired trajectory with a planar manipulator using a fixed and uncalibrated camera with image plane parallel to the task plane. The camera image coordinate frame can be related to the robot coordinate frame by the following transformation:

$$y_c = K_p y + y_{c_0}\,, \tag{1}$$

where $y_c \in \Re^2$ is the end-effector position in the image coordinate frame, K_p is the camera/workspace transformation (uncertain) matrix, $y \in \Re^2$ is the end-effector position in the robot coordinate frame, and $y_{c_0} \in \Re^2$ is a bias constant vector.

In the camera frame the cartesian control problem is described by:

$$\dot{y}_c = K_p v\,, \tag{2}$$

where $v = \dot{y}$.

A. I&I Adaptive Visual Servoing

Defining the desired trajectory y_c^* in the image frame, the tracking problem is formulated as designing v so that the tracking error $e_c = y_c - y_c^*$ tends asymptotically to zero. In order to apply the I&I Adaptive Method [22], we need to express the system (2) in a filtered version:

$$\dot{y}_{cf} = K_p v_f + \epsilon_t\,, \tag{3}$$

where

$$\dot{y}_{cf} = -\lambda_f y_{cf} + y_c\,, \tag{4}$$

$$\dot{v}_f = -\lambda_f v_f + v\,, \tag{5}$$

and ϵ_t is a vanishing term. Thus, according to [22], the control parameterization is given by:

$$v_f^* = -K_p^{-1}(\lambda_f e_{cf} - \dot{y}_{cf}^*) = \Psi_f \theta^*\,, \quad (ideal) \tag{6}$$

$$v_f = \Psi_f(\hat{\theta} + \beta_1(e_{cf}))\,, \quad (estimated) \tag{7}$$

where

$$\dot{\Psi}_f := -\lambda_f \Psi_f + \Psi\,, \tag{8}$$

$$\Psi := \begin{bmatrix} (\lambda_f e_c - \dot{y}_c^*)^T & 0 \;\; 0 \\ 0 \;\; 0 & (\lambda_f e_c - \dot{y}_c^*)^T \end{bmatrix}, \tag{9}$$

$$\Psi_f := \begin{bmatrix} (\lambda_f e_{cf} - \dot{y}_{cf}^*)^T & 0 \;\; 0 \\ 0 \;\; 0 & (\lambda_f e_{cf} - \dot{y}_{cf}^*)^T \end{bmatrix}, \tag{10}$$

$$\dot{y}_{cf}^* = -\lambda_f y_{cf}^* + y_c^*\,, \tag{11}$$

$$\dot{e}_{cf} = -\lambda_f e_{cf} + e_c\,, \tag{12}$$

$$\dot{\hat{\theta}} = -\left[2\lambda_f \Psi_f - \Psi\right]^T \Gamma^{-1} e_{cf}\,. \tag{13}$$

$$\beta_1 = -\Psi_f^T \Gamma^{-1} e_{cf}\,, \tag{14}$$

and Γ is a non-singular matrix (known) that satisfies the well-known inequality condition [8]

$$K_p \Gamma^T + \Gamma K_p^T > 0\,. \tag{15}$$

Then, defining the variable z as

$$z := \hat{\theta} - \theta^* + \beta_1\,, \tag{16}$$

the following error equations will be obtained

$$\dot{e}_{cf} = -\lambda_f e_{cf} + K_p \Psi_f z\,, \tag{17}$$

$$\dot{z} = -\Psi_f^T \Gamma^{-1} K_p \Psi_f z\,. \tag{18}$$

Now consider the quadratic Lyapunov function candidate

$$2V(e_{cf}, z) = \|e_{cf}\|^2 + \alpha \|z\|^2\,, \quad \alpha > 0\,. \tag{19}$$

Its derivative along (17) and (18) yields

$$\dot{V} = -\lambda_f \|e_{cf}\|^2 + e_{cf}^T K_p z_\psi - \alpha z_\psi^T \mathcal{M} z_\psi\,, \tag{20}$$

where

$$\mathcal{M} := \frac{1}{2}\left(\Gamma^{-1} K_p + K_p^T \Gamma^{-T}\right) = \mathcal{M}^T\,, \tag{21}$$

$$z_\psi = \Psi_f z\,. \tag{22}$$

For sufficiently large α there exists $\delta > 0$ such that

$$\dot{V} \leq -\delta(\|e_{cf}\|^2 + \|z_\psi\|^2)\,. \tag{23}$$

Thus we can state that $\lim_{t\to\infty} e_{cf}(t), z_\psi(t) \to 0$. Also, from (17) we have $\dot{e}_{cf}(t) \to 0$ and finally from (12), $e_c(t) \to 0$.

Then, restoring v from (5) we obtain the cartesian control law

$$v = \Psi\left(\hat{\theta} - \Psi_f^T \Gamma^{-1} e_{cf}\right) - \Psi_f \Psi_f^T \Gamma^{-1} e_c\,. \tag{24}$$

This is the adaptive control law to be applied in conjunction with (13).

Remark 1: In [20], a solution was proposed based on nonlinear parameterization so that only one parameter needed to be adapted, at the expense, however, of some tracking offset. For generic K_p, the present I&I approach does not lead to overparameterization, i.e., only 4 elements of K_p (6) need to be identified. This contrasts with [15] in which 5 parameters had to be identified.

III. NONLINEAR ROBOT DYNAMICS

Now consider the problem of controlling a manipulator with uncertain dynamic. The nonlinear dynamic model of the manipulator can be expressed in cartesian coordinates y by [1]

$$H(q)\ddot{y} + D(q,\dot{q})\dot{y} + W(q) = F\,, \tag{25}$$

where H, D, W are defined in terms of the joint coordinates q, $\dot{q}$, namely: $H(q) = J^{-T} M J^{-1}$, $D(q,\dot{q}) = J^{-T}(C - MJ^{-1}\dot{J})J^{-1}$, $W(q) = J^{-T}G$ and $F = J^{-T}\tau$. It is worth mentioning that in joint-space, $M(q)$ is the inertia matrix, $C(q,\dot{q})\dot{q}$ represents the centripetal and Coriolis torques, $G(q)$ represents the gravity torques, and τ is the vector of applied torques.

The properties of H and D are similar to the corresponding joint-space matrices. However, one should note that the validity of the cartesian model is restricted to motions which do not lead to a singular Jacobian matrix. We will henceforth assume that this condition holds.

The main idea of controlling robots with non-negligible and uncertain dynamic is based on a cascade control structure. Consider the cartesian control of a planar manipulator, where $y \in \Re^2$ is the cartesian end-effector coordinate vector. Assume that joint torques are such that the end-effector dynamics mimics the following simple dynamics as a reference model:

$$\dot{y}_m = -\lambda y_m + v_r\,, \tag{26}$$

where $\lambda > 0$ and $v_r \in \Re^2$ is a 2D reference signal, yet to be defined in the spirit of cascade control as in [6]. Then, if the model is followed by means of a proper design of the control law, the end-effector will behave as a linear system in response to the input v_r, i.e.,

$$\dot{y} = -\lambda y + v_r\,, \tag{27}$$

Hence, the kinematic control case considered before can be easily applied here by just letting $v_r = v + \lambda y$, where v is defined in the previous section. Thus, the problem reduces to that of achieving the tracking of the model (27), and Robust Sliding Mode Control can be used to solve this problem.

IV. ROBUST ROBOT CONTROL

It is well known from [2] that a robust control law for the forces or torques τ exists such that y will asymptotically follow y_m provided that v_r and $\dot{v}_r$ are bounded (thus yielding y_m, $\dot{y}_m$, $\ddot{y}_m$ bounded quantities). In what follows, we describe one such a robust motion controller working in cartesian coordinates. This controller is then integrated to the adaptive visual servoing algorithm developed in Section II-A. Here, it is worth mentioning that an adaptive motion controller [24] can be also used instead of the robust one.

Following [14], we define the virtual error $s \in \Re^2$ as

$$s = \dot{e} + \lambda e = \dot{y} - \dot{y}_r\,; \quad e = y - y_m\,; \quad \dot{y}_r := \dot{y}_m - \lambda e\,. \tag{28}$$

Now, define the nonnegative function

$$2V_r = s^T H s\,, \tag{29}$$

which has derivative $\dot{V}_r(s) = s^T(H\ddot{y} - H\ddot{y}_r) + \frac{1}{2}s^T\dot{H}s$. Substituting $H\ddot{y}$ by its expression obtained from the robot equation (25), one gets

$$\dot{V}_r(s) = s^T(F - H\ddot{y}_r - D\dot{y}_r - W)\,, \tag{30}$$

where the property of skew-symmetry of $\dot{H} - 2D$ has been used. In order to make $\dot{V}_r$ negative definite in s, we can take the following robust control law:

$$F = \hat{F} - \rho\frac{s}{\|s\|} - K_D s\,, \tag{31}$$

where $\hat{F}$ is some nominal control law given by $\hat{F} = \hat{H}\ddot{y}_r + \hat{D}\dot{y}_r + \hat{W}$, $K_D = diag\{k_{d1}, k_{d2}\}$ is a positive definite gain matrix and $\rho(t)$ is given as an instantaneous upper bound for the model uncertainty, such that for any constant $k_r > 0$ and $\forall t \geq 0$

$$\rho \geq \|(\hat{H} - H)\ddot{y}_r + (\hat{D} - D)\dot{y}_r + (\hat{W} - W)\| + k_r\,. \tag{32}$$

With ρ satisfying (32), $\dot{V}_r$ can be upper bounded by:

$$\dot{V}_r \leq -k_r\|s\| - s^T K_D s\,. \tag{33}$$

Thus, the inequality $\dot{V}_r \leq -k_r\|s\|$ also holds and since $V_r = (1/2)\|s\|_H^2$, it follows that V_r, and thus s, tend to zero in finite time [4, p.64]. With the expression $s = \dot{e} + \lambda e = \dot{y} - \dot{y}_m + \lambda(y - y_m)$, $v_r = \dot{y}_m + \lambda y_m$, the following expression can be derived

$$\dot{y} = -\lambda y + v_r + s\,. \tag{34}$$

Assuming that the manifold $s = 0$ has already been reached (occurs in finite time as stated above) one has y perfectly following y_m, i.e., $\dot{y} = -\lambda y + v_r$. Now, consider K_p from the camera/workspace transformation (1). Thus, in camera coordinates, after $y(t) \equiv y_m(t)$ is achieved one has $\dot{y}_c = -\lambda y_c + K_p v_r$, which is similar to the cartesian control case. Thus, it is sufficient to cascade the I&I adaptive visual servoing controller with the robust robot motion controller by simply setting

$$v_r = v + \lambda y\,, \tag{35}$$

where v is defined in (24).

However, in order to cascade the I&I adaptive controller of Section II-A with the robust one we must guarantee that the system signals remain bounded before s reaches the manifold $s = 0$. Since s appears in (34) as an input disturbance to the standard form, a new set of (disturbed) equations has to be analysed.

A. Controller Design

From (5) and

$$\dot{y}_f = -\lambda_f y_f + y\,, \tag{36}$$

$$\dot{s}_f = -\lambda_f s_f + s\,, \tag{37}$$

we can produce a filtered version of (34), say:

$$\dot{y}_f = -\lambda y_f + v_{rf} + s_f + \epsilon_t\,, \tag{38}$$

where ϵ_t is a vanishing term. Then, premultiplying (38) by K_p and assuming for simplicity that $\epsilon_t \equiv 0$, we obtain

$$\dot{y}_{cf} = -\lambda y_{cf} + K_p v_{rf} + K_p s_f\,. \tag{39}$$

Noting from (6) and (35) that

$$v_{rf} = \Psi_f\left[\hat{\theta} + \beta_1\right] + \lambda K_p^{-1} y_{cf}\,, \tag{40}$$

in order to obtain a control parameterization one has to modify slightly Ψ_f, β_1, $\dot{\hat{\theta}}$, z from (9), (14), (13), (16), respectively, as follows:

$$\bar{\Psi}_f = \begin{bmatrix} (\lambda_f e_{cf} - \dot{y}^*_{cf} - \lambda y_{cf})^T & 0 \quad 0 \\ 0 \quad 0 & (\lambda_f e_{cf} - \dot{y}^*_{cf} - \lambda y_{cf})^T \end{bmatrix} \tag{41}$$

$$\bar{\beta}_1 = -\bar{\Psi}_f^T \Gamma^{-1} e_{cf}\,, \tag{42}$$

$$\dot{\hat{\theta}} = -\left[2\lambda_f\bar{\Psi}_f - \bar{\Psi}\right]^T \Gamma^{-1} e_{cf}\,, \tag{43}$$

$$z := \hat{\theta} - \theta^* + \bar{\beta}_1\,, \tag{44}$$

yielding the following new parameterization:

$$v_{rf} = \bar{\Psi}_f\left[\hat{\theta} + \bar{\beta}_1\right]\,, \tag{45}$$

To recover the actual control v_r as done in [22], we simply resort to (24) replacing Ψ_f with $\bar{\Psi}_f$, i.e.,

$$v_r = \bar{\Psi}\left(\hat{\theta} - \bar{\Psi}_f^T\Gamma^{-1}e_{cf}\right) - \bar{\Psi}_f\bar{\Psi}_f^T\Gamma^{-1}e_c\,. \tag{46}$$

Now that (45) has been stated, we can develop (39):

$$\begin{aligned} \dot{y}_{cf} &= -\lambda y_{cf} + K_p\bar{\Psi}_f\left[\hat{\theta} + \bar{\beta}_1\right] + K_p s_f = \\ &= -\lambda y_{cf} + K_p\bar{\Psi}_f\left[z + \theta^*\right] + K_p s_f\,, \end{aligned} \tag{47}$$

where (6), (42) and (43) were used to obtain

$$\dot{e}_{cf} = -\lambda_f e_{cf} + K_p\bar{\Psi}_f z + K_p s_f\,, \tag{48}$$

$$\dot{z} = -\bar{\Psi}_f^T\Gamma^{-1}K_p\bar{\Psi}_f z - \bar{\Psi}_f^T\Gamma^{-1}K_p s_f\,. \tag{49}$$

In the particular case $s_f = 0$ the error equations (48), (49) remain essentially[1] the same as (17), (18), respectively.

[1]Except for $\bar{\Psi}_f$ instead of Ψ_f.

B. Stability Analysis

In order to verify the stability of the overall control system, we define the following quadratic full-state Lyapunov function candidate

$$2V(\xi) = \left(\|e_{cf}\|^2 + \alpha\|z\|^2 + \delta\|s_f\|^2\right) + \gamma V_r(s)\,, \quad (50)$$

where $\alpha, \delta, \gamma > 0$, $\xi = [e_{cf}^T, z^T, s_f^T, s^T]^T$ and V_r is the function defined in (29). Taking the derivative of V along the trajectories of (37), (48) and (49), follows that

$$\begin{aligned}\dot{V}(\xi) \;=\; & -\lambda_f\|e_{cf}\|^2 + e_{cf}^T K_p z_\psi + e_{cf}^T K_p s_f - \alpha z_\psi^T \mathcal{M} z_\psi \\ & -\alpha z_\psi^T \mathcal{M} s_f - \lambda_f\delta\|s_f\|^2 + \delta s_f^T s + \gamma\dot{V}_r(s)\,. \quad (51)\end{aligned}$$

with $\mathcal{M}$ defined in (21) and $z_\psi = \bar{\Psi}_f z$.

Since $\dot{V}_r(s)$ is upper bounded by (33)

$$\dot{V}_r(s) \;\leq -k_r\|s\| - s^T K_D s \;\leq -s^T K_D s\,, \quad (52)$$

we can rewrite (51) in the following compact form:

$$\dot{V}(\xi) \leq -\eta^T(\xi)\mathcal{B}\eta(\xi)\,, \quad (53)$$

where

$$\eta(\xi) = \Theta\xi\,, \quad \Theta = diag\{I,\ \bar{\Psi}_f,\ I,\ I\}\,, \quad (54)$$

and

$$\mathcal{B} = \begin{bmatrix} \lambda_f I & -\frac{1}{2}K_p & -\frac{1}{2}K_p & 0 \\ -\frac{1}{2}K_p^T & \alpha\mathcal{M} & \frac{\alpha}{2}\mathcal{M} & 0 \\ -\frac{1}{2}K_p^T & \frac{\alpha}{2}\mathcal{M} & \lambda_f\delta I & -\frac{\delta}{2}I \\ 0 & 0 & -\frac{\delta}{2}I & \gamma K_D \end{bmatrix}. \quad (55)$$

We now assume a generic block partition of $\mathcal{B}$, say

$$\mathcal{B} = \begin{bmatrix} \mathcal{B}_{11} & \mathcal{B}_{12} \\ \mathcal{B}_{21} & \mathcal{B}_{22} \end{bmatrix}. \quad (56)$$

Then, the positive definiteness of $\mathcal{B}$ will be ensured if we can satisfy the *Schur's Complement* conditions:

$$\mathcal{B}_{11} > 0\,, \quad (57)$$

$$\mathcal{B}_{22} > \mathcal{B}_{21}\mathcal{B}_{11}^{-1}\mathcal{B}_{12}\,. \quad (58)$$

So, if we first consider the choice:

$$\mathcal{B}_{11} = A = \begin{bmatrix} \lambda_f I & -\frac{1}{2}K_p \\ -\frac{1}{2}K_p^T & \alpha\mathcal{M} \end{bmatrix}, \quad (59)$$

it can be shown (*Schur's Complement* to $\mathcal{B}_{11}$) that (57) can be satisfied for all $\alpha\lambda_f > \lambda_{max}\{K_p\mathcal{M}^{-1}K_p^T\}$.

Instead, consider another choice of $\mathcal{B}_{11}$, say

$$\mathcal{B}_{11} = \begin{bmatrix} \lambda_f I & -\frac{1}{2}K_p & -\frac{1}{2}K_p \\ -\frac{1}{2}K_p^T & \alpha\mathcal{M} & \frac{\alpha}{2}\mathcal{M} \\ -\frac{1}{2}K_p^T & \frac{\alpha}{2}\mathcal{M} & \lambda_f\delta I \end{bmatrix}. \quad (60)$$

In this case, assuming that α has been fixed to a sufficiently large constant, and applying again the *Schur's Complement* to $\mathcal{B}_{11}$, we can show that it is always possible to choose δ ensuring (57), that is,

$$\delta > \lambda_{max}\left\{\begin{bmatrix} -\frac{1}{2}K_p^T & \frac{\alpha}{2}\mathcal{M} \end{bmatrix} A^{-1} \begin{bmatrix} -\frac{1}{2}K_p^T \\ \frac{\alpha}{2}\mathcal{M} \end{bmatrix}\right\}. \quad (61)$$

Here, assuming that δ has been properly fixed we can finally test (58) based on the last partition of $\mathcal{B}$. Now, since K_D is diagonal with positive entries, γ can be chosen sufficiently large to satisfy:

$$\gamma > \lambda_{max}\left\{\begin{bmatrix} 0 & 0 & -\frac{\delta}{2}I \end{bmatrix} \mathcal{B}_{11}^{-1} \begin{bmatrix} 0 \\ 0 \\ -\frac{\delta}{2}I \end{bmatrix}\right\}. \quad (62)$$

Thus, for appropriate choices of α, δ, γ in (50), the positive definiteness of $\mathcal{B}$ can be guaranteed. Although the negative definiteness of $-\eta^T(\xi)\mathcal{B}\eta(\xi)$ with respect to η is assured from the previous conclusion, only negative semi-definiteness can be stated for (53) with respect to ξ. This can be seen in (53), after restoring ξ from (54):

$$\dot{V}(\xi) \leq -\xi^T\left(\Theta^T\mathcal{B}\Theta\right)\xi \leq 0\,. \quad (63)$$

Nevertheless, based on the Lyapunov function properties of (50) and (53), we conclude that $\xi(t), \eta(t) \in \mathcal{L}_\infty$. By differentiating (53), one can verify from (37), (41), (42), (43), (48), (49) and based on *Barbalat's Lemma* that $\lim_{t\to\infty}\eta(t) \to 0$. From (48) and the conclusions above, we can state that $\lim_{t\to\infty}\dot{e}_c(t) \to 0$, which also implies that $\lim_{t\to\infty} e_c(t) \to 0$ in (12). In addition, from (50) and (63) we have that $z(t) \in \mathcal{L}_\infty$ which, consequently, leads to $\hat{\theta} \in \mathcal{L}_\infty$ in (16). Thus, we can finally conclude that all signals of the (cascade) closed loop system are uniformly bounded.

At this point, we are able to state the following result:

Theorem 1: Consider the nonlinear second order robot dynamical equation (25), the robot reference model (26) and the robust sliding mode controller (31)-(32), with v_r generated by (46) and the adaptive law (43). Under the assumptions of uniform boundedness of $\dot{y}_c^*$, y_c^* and that the Jacobian matrix J remains away from singularities, the following properties hold: (1) all signals of the closed loop system are uniformly bounded; (2) there exists some finite time t_s such that $s(t) = 0$, $\forall t \geq t_s$; (3) $\lim_{t\to\infty} e_c(t) \to 0$.

Corollary 1: Also, if y_c^* in Theorem 1 is such that $\bar{\Psi}_f$ is persistently exciting, then the full error system with state $[e_{cf}^T, z^T, s_f^T, s^T]^T$ is exponentially stable in any closed finite ball (see [14] for a proof).

Remark 2: As can be seen from the above design and analysis, the I&I method provides the use of single Lyapunov function to assert the stability of the overall cascaded system, which contrasts with some multivariable MRAC schemes (e.g. [14]). Control overparameterization is also avoided by the use of the I&I design method [22].

V. SIMULATION RESULTS

Here we consider the nonlinear second order robot dynamic model (25). Uncertainty of the robot dynamical parameters is compensated by the robust control approach developed in Section IV. If we consider that the planar two-link manipulator

$$y_1 = L_1 cos(q_1) + L_2 cos(q_1 + q_2) + O_1\,, \quad (64)$$

$$y_2 = L_1 sin(q_1) + L_2 sin(q_1 + q_2) + O_2\,, \qquad (65)$$

(where L_1, L_2 stands for link lengths, and O_1, O_2 for the base coordinates in the workspace frame) is moving on a horizontal plane (no gravity), then we have: $M_{11} = a_1 + 2a_3 cos(q_2) + 2a_4 sin(q_2)$; $M_{12} = M_{21} = a_2 + a_3 cos(q_2) + a_4 sin(q_2)$; $M_{22} = a_2$; $h_2 = a_3 sin(q_2) - a_4 cos(q_2)$; $C_{11} = -h_2\dot{q}_2$; $C_{12} = -h_2(\dot{q}_1 + \dot{q}_2)$; $C_{21} = h_2\dot{q}_1$; $C_{22} = 0$, with $a_1 = I_1 + m_1 L_{c1}^2 + I_e + M_e L_{ce}^2 + M_e L_1^2$; $a_2 = I_e + M_e L_{ce}^2$; $a_3 = M_e L_1 L_{ce} cos(\delta_e)$; $a_4 = M_e L_1 L_{ce} sin(\delta_e)$. The physical meanings of the robot parameters can be found in [2]. The parameter values were chosen to be the ones in [14], [11], say: $m_1 = 9.5\ kg$; $L_1 = 0.25\ m$; $M_e = 5.0\ kg$; $\delta_e = 0$; $I_1 = 4.3 \times 10^{-3}\ kg\ m^2$; $I_e = 6.1 \times 10^{-3}\ kg\ m^2$; $L_{c1} = 0.2\ m$; $L_{ce} = 0.14\ m$; $L_2 = 0.16\ m$; $O_1 = -0.20\ m$; $O_2 = -0.20\ m$. The desired trajectory y_c^* was designed to be the output of the model

$$\dot{y}_c^* = -y_c^* + r\,, \qquad (66)$$

in response to the external reference signals

$$r_1 = a\ sin(w_r t) + c + d\ sin(1.5 w_r t)\,, \qquad (67)$$

$$r_2 = b\ sin(w_r t + \sigma) + c + d\ sin(1.5 w_r t + \sigma)\,. \qquad (68)$$

The robust control law (31) was implemented considering $\hat{F} = 0$. Also, in order to avoid numerical problems and chattering phenomena, a smooth version based on boundary layers was used, i.e.:

$$F = -\rho \frac{s}{\|s\| + \epsilon} - K_D s\,, \quad \epsilon > 0\,. \qquad (69)$$

Note that this is not the only choice to smooth the control signal, for example, we could have considered $tanh(s/\epsilon)$ [11]. In any case these modifications could be embedded into the stability analysis resulting in convergency (Theorem 1) and exponential stability (Corollary 1) with respect to a small residual set of order ϵ (see [14] and [11]).

From the bounds of $\|H\|$, $\|D\|$, $\|J\|$ and $\|\dot{J}\|$ [14], we can define ρ as

$$\rho = \frac{\bar{M}}{|det(J)|^2} \left[\|\ddot{y}_r\| + (1 + |det(J)|^{-1}) \right] \|\dot{q}\| \|\dot{y}_r\| + k\,, \qquad (70)$$

where $\bar{M}$ is a sufficiently large constant and k is an arbitrary positive constant (eventually zero). The parameters used in the simulations were

$$K_p = \begin{bmatrix} cos(\phi) & sin(\phi) \\ -hsin(\phi) & hcos(\phi) \end{bmatrix}\,, \qquad (71)$$

$\phi = 0.5\ rad$; $h = 0.5$ (discrepancy); $\epsilon = 10^{-2}$; $\bar{M} = 20$; $k = 0$; $\Gamma = diag\{8 \times 10^{-3}, 10^{-2}\}$; $w_r = 0.5\ rad/s$; $\sigma = 1.6\ rad$; $a = b = d = 0.02$; $c = 0$; $\lambda = 1$; $\lambda_f = 10$; $K_D = diag\{2, 2\}$; $\theta(0) = [-1.5,\ 0.001,\ -0.008,\ -2.5]$.

Simulation results are presented in Figures 1 and 2. We can note from Fig. 1 that due to the small boundary layer ϵ, torque signals are continuous and free of chattering. For the sake of clarity, torque signals are shown until $t = 100\ s$. However, as can be seen also from Fig. 1, a very small residual error takes place. Indeed, the usage of larger boundary layers leads to larger residual errors [2], [4]. The image space trajectories and the adaptive parameters are presented in Fig. 2.

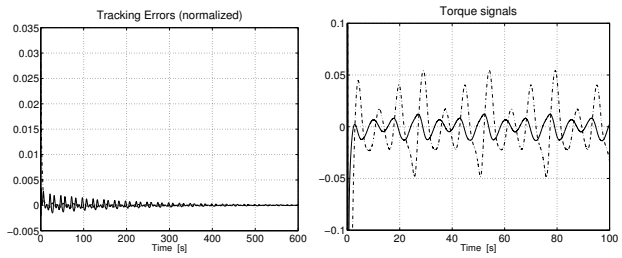

Fig. 1. Simulation results. Errors: e_{c1} (···),e_{c2} (–).Torques: τ_1(···),τ_2(–).

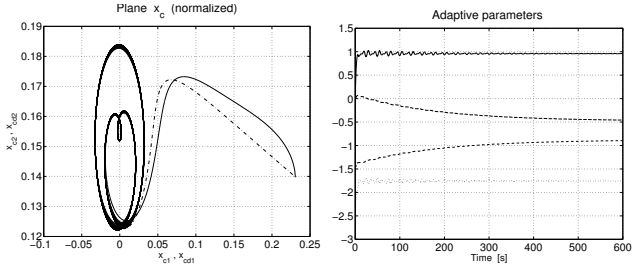

Fig. 2. Simulation results. Camera plane trajectories: x_c (–), x_{cd} (···). Adaptive parameters: θ_1 (···), θ_2 (–), θ_3 (- -) and θ_4 ($\cdots$).

VI. EXPERIMENTAL RESULTS

In this section, we describe the experimental results obtained by implementing the I&I adaptive visual servo controller proposed in Section II-A on a six d.o.f. kinematic Zebra Zero robot manipulator (IMI Inc.). A CCD camera with a lens of focal length $f = 6mm$ was mounted in front of the robot and $1\ m$ far from it. The extracted visual feature is the image coordinate of a white disc centroid located at the robot wrist. The images of 640×480 (in pixels) are acquired using a frame-grabber at 30 frames per second (FPS) with 256 grey levels. The image processing is performed on a 50×50 sub-window.

The visual servo controller was coded in C language and executed on a Pentium 200 running Linux at 35 msec. The joint velocity command generated by the adaptive control law feeds the Zebra Zero ISA board which closes the velocity loop using an HCTL1100 microcontroller (HP Inc.) working in proportional velocity mode at 0.52 msec. All tests were designed to avoid Jacobian singularities. The parameters used in the experimental tests were: $\lambda = 1$; $\lambda_f = 20$; $\Gamma^{-1} = diag\{0.0005, 0.0005\}$.

In Fig. 3 (top), tracking errors are 5 pixels of order and arise possibly due to the existence of transmission backlash in the manipulator joints. This can be also observed from Fig. 5, in which image trajectories are presented. The parameters behavior are shown in Fig. 4. The cartesian

control signals generated by the adaptive laws are also illustrated at the bottom of Fig. 3.

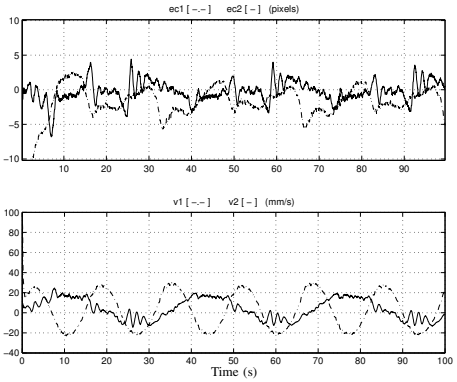

Fig. 3. Experimental results. Tracking errors e_{c1} (-··-), e_{c2} (–).

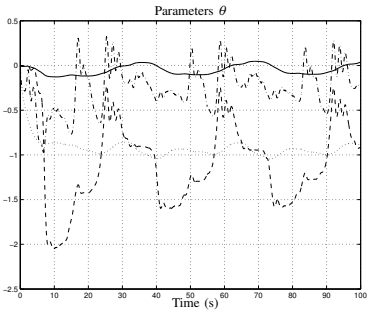

Fig. 4. Experimental results. Parameters: θ_1 (-··-),θ_2 (–),θ_3 (- -),θ_4 (· · ·).

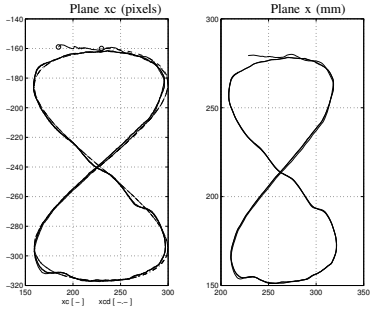

Fig. 5. Experimental results. Camera plane trajectories: x_c (–), x_{cd} (-··-).

VII. CONCLUSION

The problem of controlling robots with nonneglegible dynamics via adaptive visual servoing was presented. The proposed scheme was developed taking into account the uncertainties of both camera and robot parameters. The kinematic control for the adaptive multivariable visual servoing case was based on the recently proposed Immersion and Invariance method. The combination of the kinematic controller with the robust one was achieved by a cascade structure, resulting on an overall stable adaptive visual system. Simulation and experimental results were also presented to illustrate the performance of the proposed strategy.

REFERENCES

[1] M. W. Spong and M. Vidyasagar, *Robot Dynamics and Control*. Wiley&Sons, 1989.

[2] J. J. Slotine and W. Li, "Applied Nonlinear Control", Prentice Hall, 1991.

[3] A. Koivo and N. Houshangi, "Real-time vision feedback for servoing of a robotic manipulator with self-tuning controller", *IEEE Trans. Syst., Man, Cybern.*, vol. 21, pp. 134–142, 1991.

[4] V. I. Utkin, "Sliding Mode in Control and Optimization", Spring-Verlag, 1992.

[5] B. Espiau, F. Chaumette and P. Rives "A new approach to visual servoing in robotics", *IEEE Trans. Robotics and Automation*, vol. 8, pp. 313–326, June 1992.

[6] R. Guenther and L. Hsu, "Variable Structure Adaptive Cascade Control of Rigid-link Electrically-driven Robot Manipulator", in *Proc. IEEE Conf. on Dec. and Contr.*, (San Antonio), pp. 2137–2142, 1993.

[7] N. Papanikolopoulos and P. Khosla, "Adaptive Robotic Visual Tracking: Theory and Experiments," *IEEE Trans. Aut. Contr.*, vol. 38, no. 3, pp. 429–445, 1993.

[8] P. Ioannou and K. Sun, *Robust Adaptive Control*. Prentice Hall, 1996.

[9] P. I. Corke and M. C. Good, "Dynamic Effects in Visual Closed-Loop Systems", *IEEE Trans. Robotics and Automation*, vol. 12, no. 5, pp. 671–683, 1996.

[10] S. Hutchinson, G. Hager, and P. Corke, "A tutorial on visual servo control", *IEEE Trans. Robotics and Automation*, vol. 12, no. 5, pp. 651–670, 1996.

[11] R. Kelly, "Robust asymptotically stable visual servoing of planar robots", *IEEE Trans. Robotics and Automation*, vol. 12, no. 5, pp. 759–766, 1996.

[12] B. Bishop and M. Spong, "Adaptive calibration and control of 2D monocular visual servo systems", in *Proc. of Syroco97*, 1997.

[13] R. Kelly, F. Reyes, J. Moreno and S. Hutchinson, "Two Loops Direct Visual Control of Direct-Drive Planar Robots with Moving Target", *IEEE Int. Conf. on Robotics and Automation*, 1999.

[14] L. Hsu and P. Aquino, "Adaptive Visual Tracking with Uncertain Manipulator Dynamics and Uncalibrated Camera", in *Proc. IEEE Conf. on Dec. and Contr.*, pp. 1248–1253, 1999.

[15] E. Zergeroglu, D. Dawson, M. de Queiroz, and S. Nagarkatti, "Robust visual-servo control of robot manipulators in the presence of uncertainty", in *Proc. IEEE Conf. Dec. and Contr.*, pp. 4137–4142, 1999.

[16] L. Hsu, F. Lizarralde,"Robust Adaptive Visual Tracking Control: Analysis and Experiments", in *Proc. of the Conf. on Contr. and Applic.*,(Anchorage), 2000.

[17] L. Hsu, R. Costa, P. Aquino,"Stable Adaptive Visual Servoing for Moving Targets", in *Proc. of the American Contr. Conf.*, 2000.

[18] D. Xiao, B. K. Ghosh, N. Xi and T. J. Tarn,"Sensor Based Hybrid Position/Force Control of a Robot Manipulator in an Uncalibrated Environment", in *IEEE Trans. Contr. Syst. Techn.*,vol. 8, no. 4, 2000.

[19] L. Hsu, A. R. L. Zachi and F. Lizarralde, "Adaptive visual tracking for motions on smooth surfaces", in *Proc. IEEE Conf. Dec. and Contr.*, Orlando, Florida, 2001.

[20] A. Astolfi, L. Hsu, M. Netto and R. Ortega, "Two Solutions to the Adaptive Visual Servoing Problem", in *IEEE Trans. Robotics and Automation.*, vol. 18, no. 3, pp 387–392, 2002.

[21] Y. Fang, A. Behal, W. E. Dixon and D. M. Dawson, "Adaptive 2.5D Visual Servoing of Kinematically Redundant Robot manipulators", in *Proc. IEEE Conf. Dec. and Contr.*, Las Vegas, Nevada, pp. 2860–2865, 2002.

[22] R. Ortega, L. Hsu and A. Astolfi, "Immersion and Invariance Adaptive Control of Linear Multivariable Systems", in *Systems and Control Letters*, vol. 49, pp. 37–47, 2003.

[23] O. Nasisi and R. Carelli, "Adaptive servo visual robot control", in *Robotics and Autonomous Systems*, vol. 43, pp. 51–78, 2003.

[24] A. R. L. Zachi, L. Hsu, R. Ortega and F. Lizarralde, "Cascade Control of Uncertain Manipulator Systems Through Immersion and Invariance Adaptive Visual Servoing", in *2004 IEEE Int. Conf. on Robotics and Automation (accepted for publication)*.